

# Performance Characterization of a Small-Scale Pillow Plate Heat Exchanger Designed with the Effectiveness-NTU Method

Alessandro Dai Pré<sup>1</sup>, Luca Marchetto<sup>1</sup>, Maurizio Grigiante<sup>2</sup>

<sup>1</sup>Dept. of Industrial Engineering, University of Trento

via Sommarive 9, 38123, Trento, Italy

alessandro.daiPRE@unitn.it; luca.marchetto-1@unitn.it

<sup>2</sup>Dept. of Civil, Environmental and Mechanical Engineering, University of Trento

via Mesiano 77, 38123, Trento, Italy

maurizio.grigiante@unitn.it

**Abstract** - In recent years the design of pillow plate heat exchangers (PPHE) is attracting more and more interest both in the scientific community and in relevant industrial sectors. In this manuscript an experimental investigation has been carried out to study the thermo-hydraulic behaviour of a very compact PPHE designed in collaboration with a manufacturing company. This has allowed to design a PPHE with the smallest geometric parameters currently achievable with the present manufacturing technologies. This device mounts two pillow plates 450 mm long and 80 mm wide with an internal inflation of 3mm. In this preliminary analysis water is used as working fluid both for hot and cold channel of the PPHE which has been installed on a purpose-built laboratory-scale setup. The design of the PPHE has been carried out by implementing the efficiency-NTU number ( $\epsilon$ -NTU) method specific to PPHE geometries. The inside  $h_1$  and outside  $h_2$  heat transfer coefficients have been determined by correlations available in literature for normal types of PPHEs. The strength of the adopted approach has been verified by evaluating the errors percentage for the outlet temperatures, the efficiency and the Darcy factor referred to a wide experimental campaign. In terms of errors, the performance for predicted thermal power set from -15% to 15%, for thermal efficiency from -13% to 10%, and between 15% and 30% underestimation for the Darcy factor. The proposed procedure looks a promising engineering tool to be implemented for those applications involving small scale PPHE.

**Keywords:** Pillow Plate, Effectiveness-NTU method, Heat Exchanger, Heat transfer

## 1 Introduction

Heat exchangers (HEs) play a pivotal role in power and process industries, as well as in satellite, aviation, and micro-electronics cooling applications. The increasing demand for HEs necessitates innovative and flexible design approaches beyond traditional Shell and Tube (SHE) and Plate Heat Exchanger (PHE) designs. Recent innovations in the HEs industry can be classified into passive, active, and compound enhancements. Passive methods include special inserts into the channels or modification of the flow duct with surface extensions, thus creating swirls and vortices that enhance heat transfer coefficients. This study focuses on a specific class of passive HEs known as "Pillow Plate Heat Exchangers (PPHEs)," composed of plates, welded and hydroformed in a "pillow" shape, assembled to form two heat transfer fluid (HTF) channels within and between the inflated plates. PPHEs offer superior design flexibility, compactness, ease of installation, cost-effective production, and improved thermal efficiency and hydrodynamic performance compared to conventional HEs [1], [2]. These advantages make PPHEs attractive for applications in food industry, energy and process industries, HVAC and refrigeration, gas coolers, and distillation process HEs. Despite these benefits, PPHEs have not yet achieved the technological readiness found in conventional equipment. This is primarily because they have not been exhaustively investigated, and thus, their design procedures are not yet supported by robust and validated design tools [3].

The study of heat transfer problems in PPHEs presents valuable opportunities. The flexibility in manufacturing pillow plates allows for unlimited variations in their geometrical parameters, making PPHEs ideal for fundamental heat transfer

studies and novel design approaches, for applications involving heat transfer in the context of intensification processes. Therefore, a new PPHE configuration, designed with the smallest geometric parameters achievable using advanced technologies, was investigated. The main novelties from this study can be summarised as:

- A dedicated procedure, based on the  $\varepsilon$ -NTU method, was implemented to design and test the performance of a small-scale PPHE built for this investigation.
- Existing correlations for heat transfer coefficients and friction factors for normal PPHEs [4], [5] were applied and critically assessed for this PPHE.
- Validation tests confirmed the reliability of the proposed design approach for compact PPHEs, increasing their potential for becoming a reliable high performance heat transfer geometry.

## 2 Methodology

### 2.1 The $\varepsilon$ -NTU model for a Small Scale PPHE

The Effectiveness ( $\varepsilon$ ) – Number of Transfer Units (NTU) ( $\varepsilon$ -NTU method) is recognized as a simple and yet powerful tool for analysing the thermal performance of heat exchangers. In this work this method has been implemented within a dedicated procedure and tested as basic design tool to be applied to Small-Scale Pillow Plate Heat Exchanger (SSPPHE). This is achieved by modelling the geometry of the pillow plate through the elaborations proposed in [3] that allows to estimate, by providing as input only the macroscopic geometric parameters, the hydraulic diameters, the exchange area and further geometric parameters specific of this type of heat exchanger. All these parameters, suitably elaborated by including the inlet temperatures, the flow rates and the thermophysical properties values (in this work obtained with the Coolprop open-source database [6]), allow to determine the dimensionless numbers of Reynolds ( $Re$ ) and Prandtl ( $Pr$ ) that, correlated through empirical equations, provide the Nusselt ( $Nu$ ) number from which the heat transfer coefficient is finally obtained. The correlations for  $Nu$ , which are commonly used in the model to determine the heat transfer coefficients, were chosen by the most advised by the extensive review on PPHE by Joybary et al. [7]. The correlation  $Nu=f(Re,Pr)$  for the pillow plate inner channel (IC) consist of Eqs. 1, 2, 3 and 4 from [4]. The parameters  $a$ ,  $b$ , and  $c$  are respectively the ratio of the longitudinal pitch to the transversal pitch of the PP welding spots ( $a=2sl/st$ ), the ratio of the welding spot diameter to the transversal pitch ( $b=dsp/st$ ) and the ratio of the plate internal inflation to the transversal pitch ( $c=hi/st$ ). Eq.5, named OC2 in [7] is chosen for the outer channel (OC). The validity ranges are stated as  $1000 < Re < 8000$ ,  $1 < Pr < 150$  for the IC correlation in Eq1,  $9500 < Re < 30000$ ,  $6 < Pr < 150$  for the OC correlations in Eq. 2.

$$Nu = n3Re^{n4}Pr^{n5} \quad (1)$$

$$n3 = -0.163b + 0.711c + 0.022 \quad (2)$$

$$n4 = 0.29b - c + 0.8 \quad (3)$$

$$n5 = 0.4 \quad (4)$$

$$Nu = 0.06Re^{0.745}Pr^{0.35} \quad (5)$$

It is important to specify that after the characterisation, all the correlations proposed in [7], suitable for water, were tested and the ones proposed in this work show the lowest overall error values. The Number of Transfer Units, the effectiveness and the outlet temperatures are therefore as well determined [8],[9]. By requesting only temperatures and flow rates as process data, the  $\varepsilon$ -NTU method appears to be particularly attractive and suitable to be applied to the compact PPHE investigated in this work. The relation between  $\varepsilon$  and NTU is expressed in Eq.6, where  $C_r$  is the capacity ratio.

$$\varepsilon = 1 - \exp\left\{\left(\frac{1}{C_r}\right)NTU^{0.22}[\exp(-C_r \cdot NTU^{0.78}) - 1]\right\} \quad (6)$$

## 2.2 SSPPHE Design

To validate the E-NTU design method, a PPHE was designed to replicate a STHE geometry while minimizing production parameters according to laser welding process constraints, with the objective of providing a characterisation of the smallest pillow plate geometry possible. The model allowed to forecast the PPHE performance beforehand. To provide more insights on the performance of Nu correlations for the OC, which are scarce in literature [7], it was decided to investigate lower Re ranges. The PPHE features two plates, each measuring 450 mm in length ( $L$ ) and 80 mm in width ( $W$ ), with a thickness ( $dp$ ) of 1 mm. A rendering of the plate is shown in Fig. 1. The two-plate configuration is studied to create two ICs and three OCs. The inflated plate thickness is 5 mm ( $hi + 2dp$ ), with an internal inflation of 3 mm ( $hi$ ). The PPHE has two internal and three external channels, with a median surface distance of 8 mm. The longitudinal pitch is 18 mm ( $sl$ ), and the transversal pitch is 21 mm ( $st$ ). The welded edges, not inflated, are 3 mm ( $le$ ) long, and the welding spot diameter is 5 mm ( $dsp$ ). The compact design ensures efficient heat transfer in a small footprint, with a heat transfer area over volume ratio  $\beta=340\text{m}^2/\text{m}^3$ .

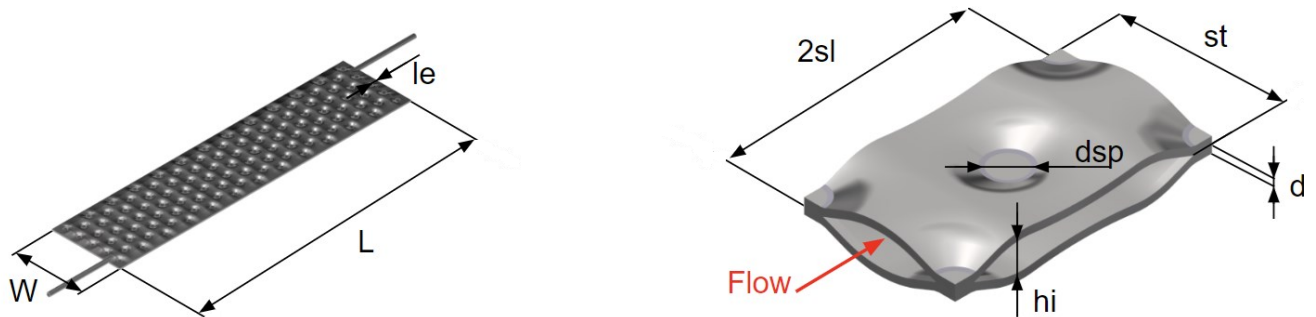


Figure 1: Pillow Plate (left) and Pillow Plate repeating unit (right) with parameters defining of the geometry

## 2.3 Experimental Setup

The experimental setup was designed to simulate steady-state operating conditions for the PPHE, including water flow systems, temperature control and measurement, pressure measurement, and flow meters. The system operates by circulating hot and cold fluids through the heat exchanger. The hot fluid is heated using an electric resistance heater and then pumped through the heat exchanger. Simultaneously, cold fluid from the reservoir circulates through the exchanger. Heat is rejected through the water which is discharged and refilled through the municipal water system, with the reservoirs providing thermal stability to the set-up. This setup enables a first iteration analysis of the heat transfer and the evaluation of the hydraulic resistance characteristics of the heat exchanger, providing valuable data for optimizing both the PPHE design and its target working conditions beside providing possible improvements as discussed in the conclusions section.

## 2.4 Heat Transfer and Pressure Drop Characterization

To characterise the SSPPHE behaviour, two distinct thermal performance characterisation campaigns were carried out, with fixed inlet temperatures (with small variations attributable to the heat sources). The tests of the first campaign, each one referred to the identification number (ID) 1&n (n states for the test number), were performed by changing the OC flow rate within the range of 0.111-0.224 kg/s and keeping the IC flow rate constant around an averaged value of 0.111 kg/s. Conversely, the second campaign, with ID2&n, was performed by changing the IC flow rate in the range of 0.042-0.330 kg/s. The OC flow rate was set at an average value of 0.180 kg/s. As for the inlet temperature of the fluids ( $T1i$  for IC and  $T2i$  for OC), the average value was  $T1i=324.11\text{K}$ ,  $T2i=287.77\text{K}$  for the campaign ID1&n,  $T1i=323.77\text{K}$  and  $T2i=285.57\text{K}$  for ID2&n.

Pressure drop was measured in both the inner and outer channels of the SSPPHE. However, since the pressure drop in the outer channel was unexpectedly below the sensor's accuracy, only data for the inner channel are here reported. To isolate the pressure loss within the pillow plates, the pressure drop in the connections was computed using the Blasius correlation, as described in [10]. The pressure drop relationship with the flow regime is evaluated throughout the Blasius equation, that

correlates the Darcy friction factor ( $\xi$ ) and Re number, shown in Eq. 7. As seen in Eq. 8-9, both  $\xi$  and Re depend from the hydraulic diameter ( $Dh$ ) and the velocity of the flow ( $v$ ), which is calculated by dividing the volumetric flow rate by the fluid passage area ( $Acs$ ). To determine  $Dh$  and  $Acs$  from the main geometrical features of the pillow plate, two different approaches from literature were selected: one from Arsenyeva et al. [11] (also referred in this text as Arsenyeva's method), a relevant SSPPHE investigation work, and another from Piper et al. [3] (also referred in this text as Piper's method), which is used in the design  $\varepsilon$ -NTU\_model to determine the internal volume ( $V$ ), heat transfer area,  $Dh$ , and other relevant geometrical parameters. The mass flux rate ( $\varphi$ ) was also computed to display pressure drop against different flow conditions and is obtained from the volumetric flow rate ( $Q$ ), the density at mean temperature ( $\rho$ ) and  $Acs$ . However, since this PPHE is even smaller, a significant deviation from the available geometrical models was expected and had to be determined before analysing data from the pressure drop analysis.

$$\xi_{Darcy} = n1 \cdot Re^{n2} \quad (7)$$

$$\xi_{Darcy} = \frac{2 \cdot \Delta P \cdot Dh}{\rho \cdot v^2 \cdot L} \quad (8)$$

$$Re = \frac{v \cdot Dh}{\mu} \quad (9)$$

$$\varphi = \frac{Q \cdot \rho}{Acs} \quad (10)$$

$$Dh = \frac{4 \cdot Volume}{Area_{wetted}} \quad (11)$$

## 2.5 Passage Area Measurements

To evaluate theoretical  $Acs$  values, the pillow was cut to expose the cross-sectional area at specific points where it is at the minimum and maximum. Images were then captured with a calibrated microscope at low magnification, and a computer vision algorithm was applied to measure the area in the pictures, providing a reference range for minimum and maximum area. To validate these measurements, the inner channel was filled with distilled water, and the pillow was weighed before and after being filled, to determine the weight gain. Knowing the specific density of water at 20°C, the inner volume was computed. By dividing the volume by ( $L-2le$ ),  $Acs$  can be determined, following the approach of calculating the cross-sectional area by dividing the volume element per its length (the longitudinal semi-pitch)[3]. The hydraulic diameter was determined using Eq.11, with the wet area ( $Area_{wetted}$ ) calculated by the SSPPHE design model which implements the approach from Piper et al. [3]. These values are important as they allow to check the difference between the computed values, which apply to an infinitely extended pillow plate surface with negligible border effects, and the real values of the studied small scale pillow plate with the same set of geometrical parameters.

## 3 Experimental Results and discussion

### 3.1 Pressure Drop Study

For the characterization of the pressure drop in the Inner Channel (IC) of the Small-Scale Pillow Plate Heat Exchanger (SSPPHE), experiments were conducted over a mass flow ranging from 0.042 to 0.330 kg/s. The temperature in the IC was intended to be constant, but minor variations due to system instabilities resulted in a mean temperature range of 313.15-320.15 K. The Outer Channel (OC) maintained a temperature range of 288.15-290.15 K. The obtained value for average measured area from the volume of contained water and the wet area, is 118.36 mm<sup>2</sup> (water density at 20°C was considered 998.29 kg/m<sup>3</sup>). This value is validated against the range defined by the minimum and maximum values of the area measured from the images, which are 77.60 mm<sup>2</sup> and 148.60 mm<sup>2</sup>. From the images *hi*, was found to have a maximum and a minimum

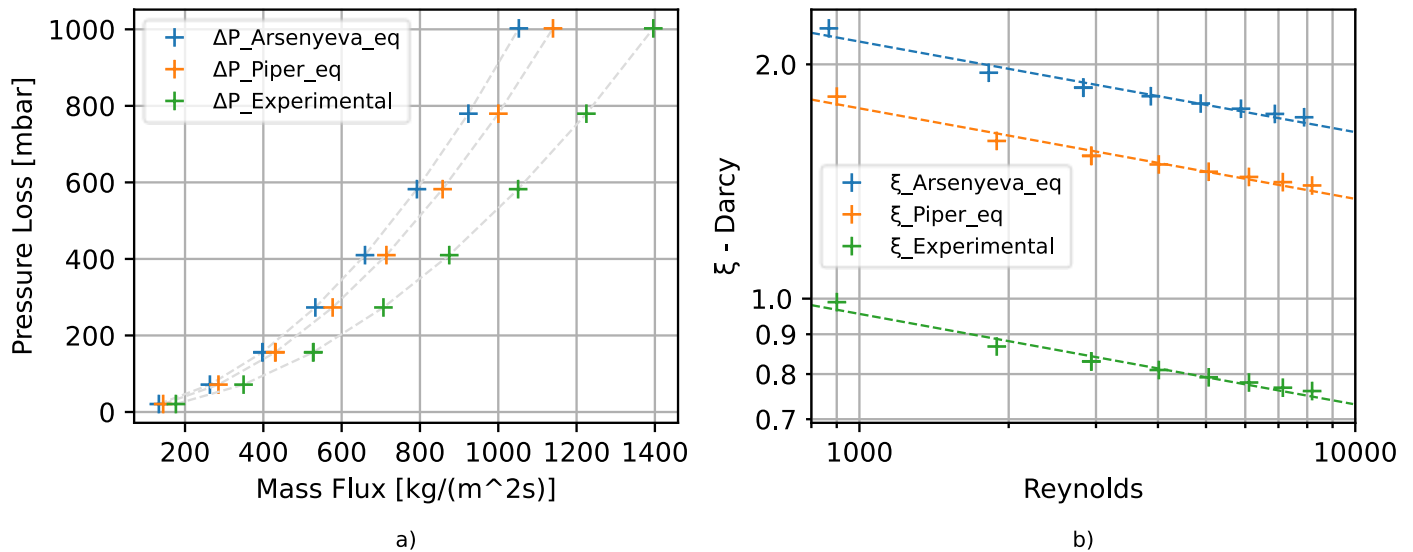


Figure 2: Representation of a) pressure drop data against mass flux; b) Darcy friction against Reynolds number. Both diagrams present different curves from the same data, analyzed with different values for hydraulic diameter and passage area of the PPHE. Sets of points and curves, from top to bottom, blue to green, are respectively calculated with quantities from references [3],[11] and experimental values from this work.

of 2.99 mm and 2.52 mm: the former value indicates a good agreement with the nominal  $hi$  value, but also local deviations from it. The corresponding  $D_h$  values were 4.24 mm (Arsenyeva’s method), 4.06 mm (Piper’s method), and 3.32 mm calculated from the destructive testing (later referred to as “experimental parameters”).

Using the pressure drop data and the determined cross-sectional areas and hydraulic diameters, the Reynolds number, mass flux, and Darcy factor were computed. Figure 2a illustrates the relationship between the pressure drop in the IC and mass flux, while Figure 2b presents the computed Darcy factor for the three different approaches. Based on the measured points, three different fitting curves were computed using Eq. 7. The resulting curves are shown in Figure 3, with the coefficients of Eq. 7 found to be:  $n_1=4.778$  (blue line – Arsenyeva’s method),  $n_1=3.922$  (orange line – Piper’s method), and  $n_1=2.135$  (green line – experimental parameters), while  $n_2=-0.116$  for all curves. These results are significantly influenced by the computed areas and hydraulic diameter, underscoring the importance of accurate measurements. Figure 2a shows the pressure drop in the IC plotted against mass flux, and Figure 2b shows the computed Darcy factor against Reynolds number. These figures demonstrate the influence of the calculation method on the pressure drop and Darcy factor curves. Figure 2a indicates higher mass flux numbers for the lower computed area at a given pressure drop value, while Figure 1b suggests that the actual passage area and hydraulic diameter are significantly lower than those calculated by the geometrical correlations. The curves in Figure 2b are, at a given Reynolds number, too high compared to all available pressure drop data on PPHEs [7]. The experimental results were then compared by plotting the computed Darcy factor using Eq. 8 against the analytical results derived from the method in [11]. Figure 3a shows four curves derived in [11] for significant PPHE geometries in the literature, and an orange curve representing the correlation presented in [11] but calculated for the SSPHE in this study. This is the curve the measured data is expected to fit. The blue cross marks on the plot represent the experimental Darcy values, derived from pressure measurements and the average area and hydraulic diameter obtained from experimental destructive testing explained in section 2.5. Figure 3b provides a direct comparison between the experimental Darcy values and those computed using the method from [11] with the pillow parameters from this study at the same Reynolds numbers. This plot shows a deviation of up to 30% from equality, which can be attributed to the border effect not considered by current geometrical models [3], [11], and the averaging technique used in this study, which does not account for the flow regime near the narrowly inflated borders of the internal channel of the SSPHE.

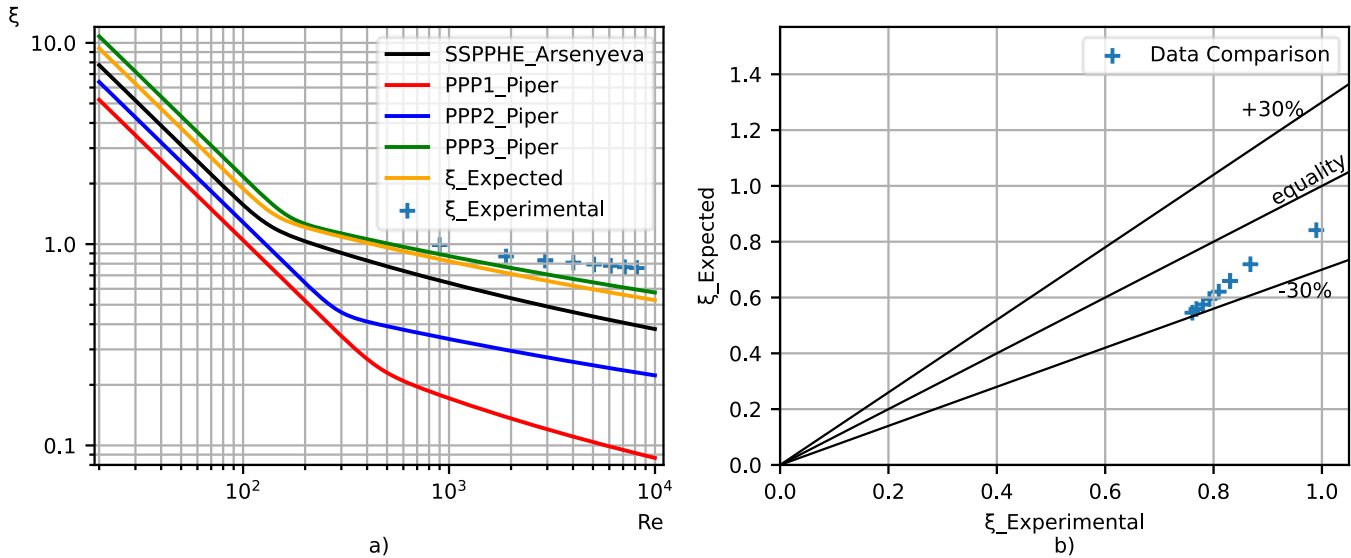


Figure 3: Comparison of Darcy values from experimental data, determined with experimental hydraulic diameter and cross-sectional areas from this study. In Fig. 2a) the Experimental data points are plotted against curves drawn with the SPPHE correlation for Darcy presented in [11] and the same correlation including the geometrical parameters of this study ( $\xi_{Experimental}$ ). Fig. 2b) Directly compares the experimental values for the Darcy friction factor and the ones determined with the approach proposed in [11]

### 3.2 SPPHE Characterization and $\epsilon$ -NTU model performance evaluation.

The data set presented by Table 1 reveals critical insights into the behaviour of the heat exchanger across two experimental campaigns. In the first campaign, the IC conditions were kept constant, and the OC Reynolds numbers ( $Re_2$ ) are varied (524 to 1807), leading to a wide range in the thermal resistance of the OC. In the second campaign, Reynolds number is varied only in the internal channel. The moderate deviation between experimental and calculated overall heat transfer coefficient values reported in Table 1, suggest the onset of turbulence at low Reynolds number for both the OC and IC of the SPPHE. It is generally possible, across the dataset, to appreciate the general fidelity of the predictions of the model, but also some variability in the stability of the experimental system, since the non-adiabaticity (%NA) does not seem to correlate to the flow regime and thermophysical property variation. In Figure 4, two relevant output values predicted by the  $\epsilon$ -NTU model are plotted against the measured values of two key output parameters of the SPPHE: the thermal power, and the outlet temperature for both the inner and outer channel. The comparison of computed vs. measured output powers, as depicted in Figure 4a, provides critical insights into the performance and accuracy of the  $\epsilon$ -NTU model for the PPHE. The  $\epsilon$ -NTU model demonstrates accuracy within specified Reynolds ( $Re$ ) and Prandtl ( $Pr$ ) number ranges but exhibits higher deviations when applied increasingly outside these ranges, particularly in the OC. In Figure 4a it is also possible to see separate points for IC (hot fluid) and OC (cold fluid), with the gap related to the non-adiabaticity ( $NA$ ). Positive deviations indicate underestimation of a computed parameter.

IDs 1&1 and 1&2 show significant positive deviations (13.65%, 15.26%) with  $Pr_2$  values that are close to the lower limit valid range. High deviations are also observed in the second experimental run for IDs 2&9 (6.53%) and 2&7 (5.68%), indicating underestimation at higher Reynolds numbers in the inner channel.

Negative Deviations indicate overestimation by the model, and IDs 1&3, 1&4, and 1&5 exhibit negative deviations (-6.80%, -9.13%, -8.01%) despite being within the valid range for  $Re_1$ , most likely due to error from OC low  $Re$  conditions. ID 2&1 ( $Re_1 = 914$ ) shows a -7.53% deviation: since the Reynolds value for the IC is below the valid range of the Nusselt correlation, it is possible to confirm reduced accuracy outside the specified ranges. In Figure 4b, deviation in the prediction of outlet temperatures is shown, completing the information from Figure 4a. The deviations are much smaller for the predicted outlet Temperatures, which is to be expected since both the computed power and the measured power are derived from the Temperature differences, the specific heat, and the measured flow rates.

Table 1: Summary of key parameters of influence for performance evaluation: effectiveness ( $\epsilon$ ), global heat exchange coefficient (U), Non-adiabaticity (NA), Reynolds (Re) and Prandtl (Pr) numbers calculated by the presented  $\epsilon$ -NTU model, heat exchange coefficients (h) calculated by the model, Power (P). The subscript “exp” is for values calculated from experimental data, “comp” is for parameters computed by the model, while 1 and 2 indicate the inner (hot) and outer (cold) channel.

ID	$\epsilon_{exp}$ (%)	$\epsilon_{comp}$ (%)	$U_{exp}$ (W/m <sup>2</sup> K)	NA (%)	Re1	Re2	Pr1	Pr2	h1 (W/m <sup>2</sup> K)	h2 (W/m <sup>2</sup> K)	$U_{comp}$ (W/m <sup>2</sup> K)	$P_{comp}$ (W)
1&1	36.78	33.81	919	4.25	2649	524	3.73	6.51	814	936	814	2727
1&2	28.13	25.41	1410	3.97	2657	1000	3.87	6.88	1218	1537	1218	4160
1&3	23.93	27.12	1132	5.31	2737	1121	3.82	7.42	1321	1703	1321	4736
1&4	26.86	30.09	1270	1.78	2705	1351	3.86	7.62	1471	1970	1471	5316
1&5	31.09	34.7	1492	2.57	2663	1807	3.93	7.8	1718	2460	1718	6180
2&1	50.83	56.04	1039	1.92	914	1269	4.26	8.09	4056	1909	1204	3759
2&2	35.34	37.61	1292	2.63	1904	1327	4.02	7.91	6794	1962	1399	4982
2&3	27.19	28.13	1440	3.82	2947	1354	3.91	7.8	9249	1984	1495	5605
2&4	27.19	28.02	1437	1.59	2945	1346	3.92	7.82	9252	1977	1491	5564
2&5	21.91	22.42	1515	3.8	4026	1368	3.83	7.73	11528	1995	1552	5991
2&6	23.24	23.31	1578	1.93	5071	1368	3.76	7.62	13552	1989	1581	6219
2&7	23.76	23.93	1602	6.04	6112	1368	3.74	7.64	15502	1990	1606	6395
2&8	25	24.49	1668	0.9	7150	1370	3.73	7.6	17354	1990	1624	6472

Given that the highest thermal resistance is in the outer channel, it can be stated that the overall thermal resistance is closer to its value. However, the model's predictions are reliable within a 15% deviation, allowing the outer channel correlation to be used down to  $Re = 1000$ , thereby extending its applicability. This extension is significant for designing heat exchangers operating under varied flow conditions, ensuring robust thermal performance predictions.

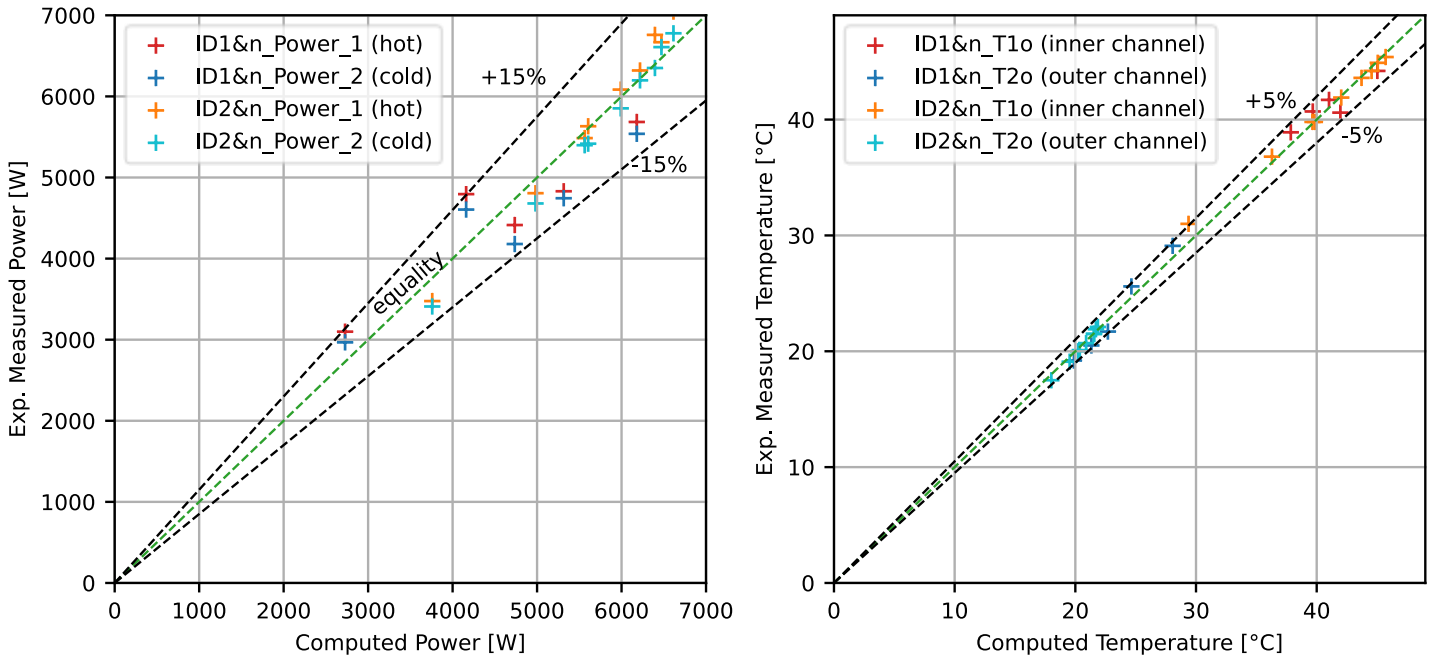


Figure 4: Comparison between a) the computed power and b) the computed temperature, against the respective measured value. Positive deviation from equality corresponds to underestimation of the quantity by the model.

## 4 Conclusions

This work investigates the accuracy of a design procedure based on the  $\varepsilon$ -NTU method to evaluate the hydro-thermal performances of a compact PPHE. The predictions of the model align well with the experimental data within acceptable errors ranges. Future works will be focus on extending the experimental activities and enhancing the methodology pertaining to the calculation of the geometrical parameters. Considering the global performances referred to the actual state of the study, the obtained model can be used for a preliminary evaluation of PPHH design.

## Acknowledgements

The authors would like to express their gratitude to DavCoil srl for supporting this project with the construction of the SSPHE and the acquisition of new instrumentation for the experimental runs. Special thanks are also extended to Dr. Mauro Hueller, Dr. Francesco Negrisolo and Dr. Raffaele De Biasi who provided invaluable assistance in the experimental work.

## 5 References

- [1] R. Eldeeb, J. Ling, V. C. Aute, and R. Radermacher, 'Heat Transfer Enhancement Using Approximation Assisted Optimization for Pillow Plate Heat Exchangers', 2018.
- [2] J. Mitrovic and B. Maletic, 'Numerical Simulation of Fluid Flow and Heat Transfer in Thermoplates', *Chem. Eng. Technol.*, vol. 34, no. 9, pp. 1439–1448, Sep. 2011, doi: 10.1002/ceat.201100271.
- [3] M. Piper, A. Olenberg, J. M. Tran, and E. Y. Kenig, 'Determination of the geometric design parameters of pillow-plate heat exchangers', *Appl. Therm. Eng.*, vol. 91, pp. 1168–1175, Dec. 2015, doi: 10.1016/j.applthermaleng.2015.08.097.
- [4] M. Piper, A. Zibart, and E. Y. Kenig, 'New design equations for turbulent forced convection heat transfer and pressure loss in pillow-plate channels', *Int. J. Therm. Sci.*, vol. 120, pp. 459–468, Oct. 2017, doi: 10.1016/j.ijthermalsci.2017.06.012.
- [5] O. Arsenyeva, J. Tran, M. Piper, and E. Kenig, 'An approach for pillow plate heat exchangers design for single-phase applications', *Appl. Therm. Eng.*, vol. 147, pp. 579–591, Jan. 2019, doi: 10.1016/j.applthermaleng.2018.08.083.
- [6] I. H. Bell, J. Wronski, S. Quoilin, and V. Lemort, 'Pure and Pseudo-pure Fluid Thermophysical Property Evaluation and the Open-Source Thermophysical Property Library CoolProp', *Ind. Eng. Chem. Res.*, vol. 53, no. 6, pp. 2498–2508, Feb. 2014, doi: 10.1021/ie4033999.
- [7] M. Mastani Joybari, H. Selvnes, A. Sevault, and A. Hafner, 'Potentials and challenges for pillow-plate heat exchangers: State-of-the-art review', *Appl. Therm. Eng.*, vol. 214, p. 118739, Sep. 2022, doi: 10.1016/j.applthermaleng.2022.118739.
- [8] D. P. Sekulic', R. K. Shah, and A. Pignotti, 'A Review of Solution Methods for Determining Effectiveness-NTU Relationships for Heat Exchangers With Complex Flow Arrangements', *Appl. Mech. Rev.*, vol. 52, no. 3, pp. 97–117, Mar. 1999, doi: 10.1115/1.3098928.
- [9] R. Sukarno, N. Putra, I. I. Hakim, F. F. Rachman, and T. M. I. Mahlia, 'Multi-stage heat-pipe heat exchanger for improving energy efficiency of the HVAC system in a hospital operating room1', *Int. J. Low-Carbon Technol.*, vol. 16, no. 2, pp. 259–267, May 2021, doi: 10.1093/ijlct/ctaa048.
- [10] A. Celen, A. S. Dalkilic, and S. Wongwises, 'Experimental analysis of the single phase pressure drop characteristics of smooth and microfin tubes', *Int. Commun. Heat Mass Transf.*, vol. 46, pp. 58–66, Aug. 2013, doi: 10.1016/j.icheatmasstransfer.2013.05.010.
- [11] O. Arsenyeva, M. Piper, A. Zibart, A. Olenberg, and E. Y. Kenig, 'Investigation of heat transfer and hydraulic resistance in small-scale pillow-plate heat exchangers', *Energy*, vol. 181, pp. 1213–1224, Aug. 2019, doi: 10.1016/j.energy.2019.05.099.